Materials Research Proceedings **4** (2018) 123-128 doi: http://dx.doi.org/10.21741/9781945291678-19

Depth-Resolved Strain Investigation of Plasma Sprayed Hydroxyapatite Coatings Exposed to Simulated Body Fluid

T. Ntsoane[1,2,a*], C. Theron[2,b], M. Topic[3,c], M. Härting[4,d] and R. Heimann[5,e]

[1]Research and Development Division, Necsa SOC Limited, Pretoria, South Africa

[2]Department of Physics, University of Pretoria, Pretoria, South Africa

[3]Materials Research Department, iThemba LABS/National Research Foundation, Cape Town, South Africa

[4]Department of Physics, University of Cape Town, Cape Town, South Africa

[5]Am Stadtpark 2A, D-02826 Görlitz, Germany

[a]tshepo.ntsoane@necsa.co.za, [b]chris.theron@up.ac.za, [c]mtopic@tlabs.ac.za, [d]margit.harting@uct.ac.za, [e]robert.heimann@ocean-gate.de

Keywords: Plasma-Sprayed Hydroxyapatite Coatings, In-Vitro Investigation, High-Energy Diffraction, Residual Stress

Abstract. The influence of exposure to simulated body fluid (SBF) on plasma sprayed hydroxyapatite (HAp) coatings on medical grade Ti6Al4V samples has been investigated. Through-thickness residual strain investigations of HAp coatings deposited on flat substrate surfaces incubated for 7, 28 and 56 days were performed using high-energy synchrotron diffraction techniques. In the as-sprayed condition, the results show the top half of the HAp coating to be under compression with the maximum around the near-surface region, relaxing with depth below the surface reaching a strain-free point around the coating thickness midpoint. On the contrary, the remainder of the coating is under tension increasing with further depth; the maximum tension is observed near the coating-substrate interface region. Upon immersion in SBF, both the slope of the normal strain components ε_{11} and ε_{33} relax, with the former experiencing a change in slope before saturating after 7 days; the highest change was observed within the first week of incubation.

Introduction

The second-generation biomaterial hydroxyapatite (HAp) has been extensively studied as a candidate material in biomedical applications due to its similarity to the mineral component of bone. These include filling of bone cavities [1] and medical implant coatings for improved biological fixation [2] amongst others. The poor mechanical properties of the material, however, limit its bulk utilisation in load-bearing applications. To overcome this limitation, the material is applied as a coating on metallic substrates such as Ti, Ti alloys and CoCrMo, combining the excellent mechanical properties of the metal with the osseoconductive ability of the coating [3]. With the plethora of coating techniques available for deposition [4], thermal spraying is still the method of choice. Although successfully utilised at an industrial scale (see, for example [5]), the high plasma temperature together with the cold substrate surface that the droplet impinges on, generally results in thermal decomposition of the HAp powder and rapid cooling on the substrate respectively. This leads to the introduction of undesirable thermal decomposition products [6], such as tricalcium phosphate (TCP), tetracalcium phosphate (TTCP), and sometimes calcium oxide as well as a reduced crystallinity [7]. These products are known to be susceptible to dissolution in simulated body fluids [8] and thus together with the strains and stresses generated

Materials Research Proceedings **4** (2018) 123-128 doi: http://dx.doi.org/10.21741/9781945291678-19

as a result of differential thermal mismatch (CTE) and quenching of the droplet, may compromise the mechanical stability and integrity of the coating. Although extensive investigation of the effect of incubation of HAp coatings in simulated body fluid have been carried out by many research groups around the world [6], the bulk of their work focused on the near-surface region coating, i.e. the region in immediate contact with living tissue. The present study is an extension of the author's previous work [9] on through-thickness investigation of HAp coating in the as-sprayed condition.

Materials and methods

Sample preparation: Hydroxyapatite powder (CAPTAL 90, batch P215, Plasma Biotal Limited, Tideswell, Derbyshire, UK) with size distribution of 120 ±20 μm was plasma-sprayed onto flat discs of 20 mm diameter medical grade Ti6Al4V alloy substrate supplied by Biomaterials Limited, North Yorkshire, UK. Details of deposition and spray parameters have been reported elsewhere [9]. Subsequent to spraying, the samples were incubated in simulated body fluid for 7, 28 and 56 days to mimic the physiological environment. Sample incubation was carried out in a revised simulated body fluid (rSBF) based on Kokubo's formulation [10]. The solution had an ionic concentration similar to the human blood plasma but without proteins and enzymes. The temperature and *pH* of the solution during incubation experiment were kept at 36°C and *7.4*, respectively. Subsequent to immersion, slices of approximately 5 mm thick were cut for investigation. Factors considered in determining the optimum slice length are reported elsewhere [9].

Through-thickness characterisation of HAp coating: Angular dispersive diffraction measurements utilising the high–energy synchrotron radiation, 100 keV (wavelength λ = 0.12331 Å), at the Advanced Photon Source's X-ray Operation and Research 6-ID-D beamline at Argonne National Laboratory , USA was used for the experiments. Experimental details and measurement procedure have been reported elsewhere [9]. Measurements were done in transmission geometry using a 35(V) x 400 (H) μm^2 beam and for one azimuth orientation hence the full strain tensor was not measured. The analysis of the data for phase composition and strain was done using TOPAS [11] and the traditional one-dimensional method [12] respectively. The error calculation in the latter was based on the standard deviation of the fit assuming a Gaussian distribution.

Cross-section microstructure examination of the as-sprayed and sample subjected to immersion in simulated body fluid was done using scanning electron microscope. For better quality micrographs, the samples were metallographically prepared and images obtained in secondary electron (SE) mode.

Results and discussion

Phase analysis: Fig.1 show the superposed diffraction patterns of the as-sprayed and the sample immersed the longest (56 days) as well as the corresponding volume fractions of the starting HAp phase and main thermal product (TTCP) collected at different depths below the coating surface; the bottom patterns in the former represent the shallow depths probed in this geometry. The last top diffraction pattern(s) in the figures corresponds to the Ti alloy indicating that probing extended beyond the coating-substrate interface. The high temperature induced thermal products TTCP, TCP, and CaO can be seen through-out the as-sprayed coating, see Fig. 1a. Upon immersion these phases dissolve, with the latter being first to disappear. After 56 days of immersion, CaO has almost completely disappeared while TTCP and TCP only start appearing deeper in the coating see Fig. 1b.

Materials Research Proceedings **4** (2018) 123-128 doi: http://dx.doi.org/10.21741/9781945291678-19

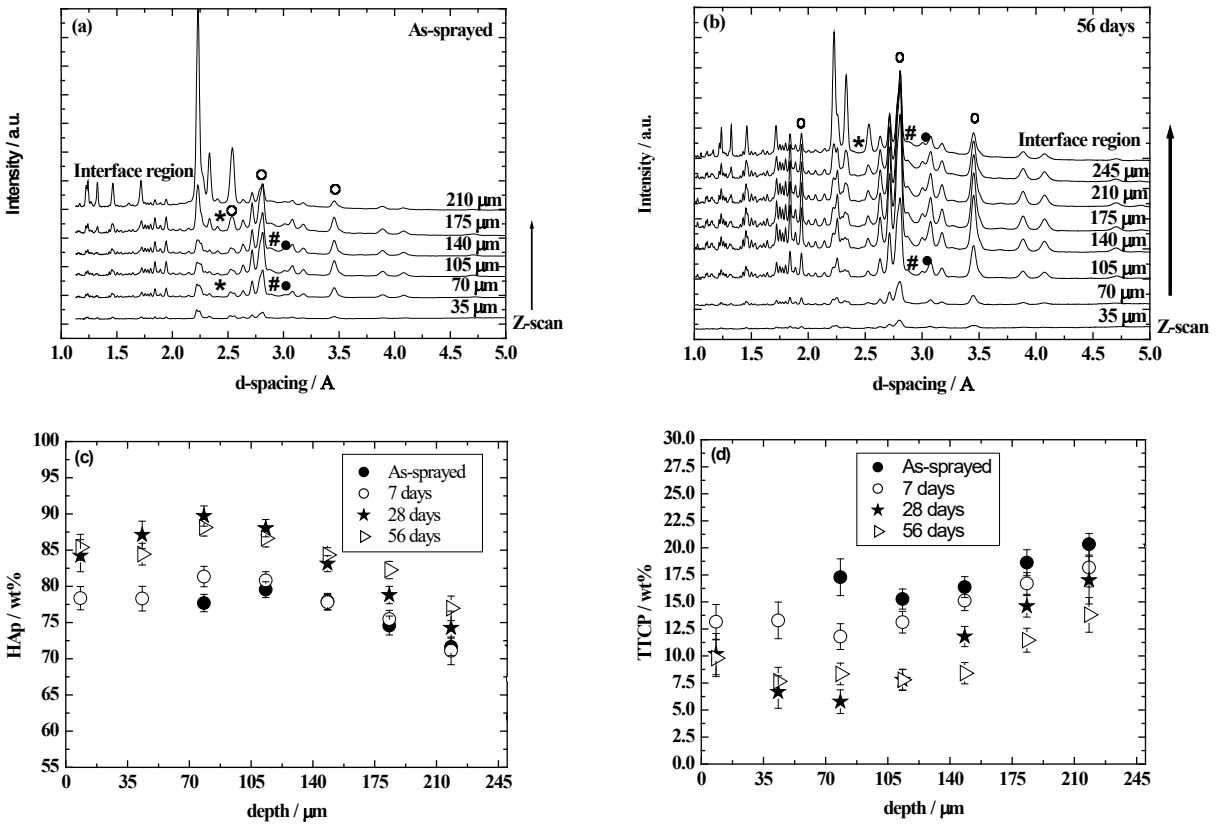

Fig. 1: Through-thickness diffraction patterns of HAp coatings: (a) as-sprayed, (b) 56 days immersed samples showing the presence of HAp (o), TTCP (#), TCP (•) and CaO (*) and the corresponding volume fractions: (c) HAp and (d) TTCP.

The corresponding volume fraction for the HAp phase as well as the main thermal product, TTCP for all immersion periods are shown in Figs. 1c and d. For the as-sprayed condition, HAp increases linearly with depth from ~75 wt.% at the near-interface region to a maximum of 80 wt.% at around 105 µm before decreasing to ~77 wt.% near the coating surface. The observed reduction in HAp closer to the coating surface might be attributed to slower cooling rates towards the outside of the layer due to the already elevated temperature and the lower thermal conductivity of HAp. Upon immersion the amount of HAp increases gradually reaching a maximum around 28 days of immersion. The observed relative increase is be attributed to the dissolution of thermal products from the coating into the solution, leaving behind a more stable HAp phase. An opposite trend is observed for the thermal product TTCP in the as-sprayed condition, decreasing from ~22.75 wt.% at the interface region reaching a minimum of ~15 wt.% before increasing near the coating surface. It decreases further upon immersion.

Microstructure: Fig. 2 shows the SEM micrographs of the as-sprayed and SBF immersed coatings. In general the micrographs show a laminar-based structure indicative of the splat-based nature of the coating. The interface region of the as-sprayed coating shows a slightly higher number of partially and/ or unmolten particles, Fig. 2a. The fine-grained equiaxial microstructure revealed by microscopy is an indication of low heat removal from the deposited splats. This is to be expected given the already elevated substrate temperature due to heat flux from the plasma jet and the already deposited HAp splats. Additionally, the presence of high concentration of splat boundaries, fine boundaries and gaps/pores resulting from poor adhesion between the splats can be seen, as well as cracks resulting from in-plane residual stresses. Upon immersion the laminar

Materials Research Proceedings **4** (2018) 123-128 doi: http://dx.doi.org/10.21741/9781945291678-19

structure is replaced by very fine grains, as well as nano-sized pores resulting in an increased coating porosity. The latter connects with one another resulting in a 3D network of dissolution channels which facilitate dissolution deeper in the coating. With further immersion , an apatite-like precipitate layer (of thickness ~20 μm) is formed on the coating surface, Fig. 2b. Closer examination of the micrograph reveals that the precipitate is not only limited to the coating surface but extends into the bulk, thereby filling some pores.

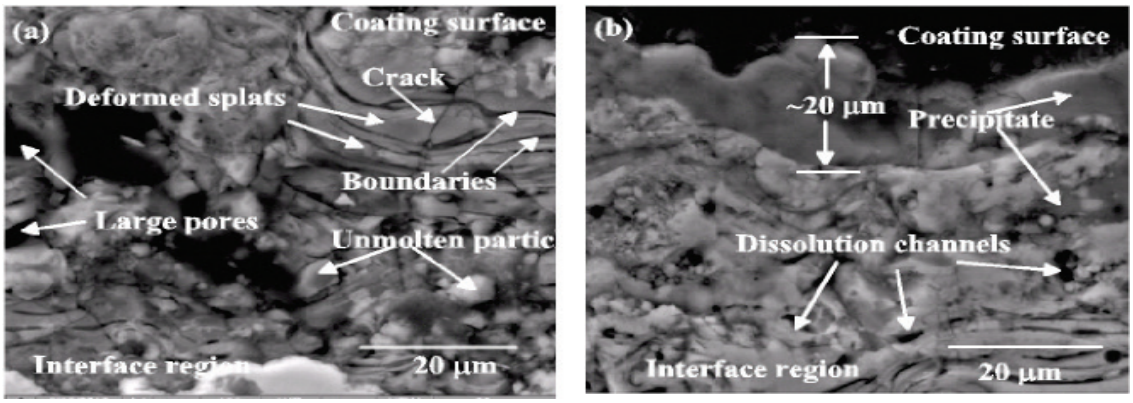

Fig. 2: Cross-section morphology of HAp coating for different immersion times: a) as-sprayed and b) 56 days. The latter indicates presence of a layer of apatite-like precipitate.

Residual strain: Figs. 3a and 3b show the through-thickness normal strain components ε_{11} and ε_{33} of the coatings for the different immersion periods respectively. The values are calculated from the 213 reflections of the main phase HAp with the stress-free reference d-spacing d_0 determined from the powder prepared from sprayed coating flakes. This was done to ensure that the observed changes were due to residual stress and not chemistry changes induced by spraying. The observed plots show the strain in the as-sprayed condition to be generally small with the normal component ε_{11} under tension in the first half of the coating. It relaxes linearly with depth below the coating surface reaching a strain-free point around the coating midpoint from which a change in strain state is observed. An opposite trend is observed for the normal component ε_{33}. Dissolution behaviour corresponding to the slope of the fits to the data points, $\Delta\varepsilon_{ij}$ as a function of immersion time are summarised in Figs. 3c and 3d. From the figures the slope of the strain component $\varepsilon_{11,}$ $\Delta\varepsilon_{11}$ relaxes to zero before turning positive after 7 days, remaining constant with further immersion. On the other hand, the slope for the strain component $\varepsilon_{33,}\Delta\varepsilon_{33}$ relaxes linearly with depth to zero after 56 days of immersion in SBF. The observed $\Delta\varepsilon_{11}$ behaviour (in this study) is similar to the one for the coating deposited on a cylindrical rod geometry, however this is not the case for $\Delta\varepsilon_{33.}$ The latter showed significant relaxation from positive to zero in the first 7 days before stabilizing with further immersion.The observed relaxation and/or change in strain state can be attributed to dissolution of the thermal products and the amorphous content in the coating leaving behind a more stable crystalline HAp, as well as the formation of apatite-like precipitate.

The observed as-sprayed distribution trend is consistent with the findings of Cofino *et al.* [13]. A combination of the high quenching effect upon droplet impact on cooler substrate and slightly higher thermal expansion coefficient of the coating as compared to the substrate are attributed to the higher coating tension at the interface region. The observed strain relaxation and change in strain state i.e. from compression to tension, upon immersion is attributed to the dissolution of thermal products and precipitate layer formed. The observed change in strain/stress state upon SBF immersion is consistent with Nimkerdphol *et al*. [14].

Materials Research Proceedings **4** (2018) 123-128 doi: http://dx.doi.org/10.21741/9781945291678-19

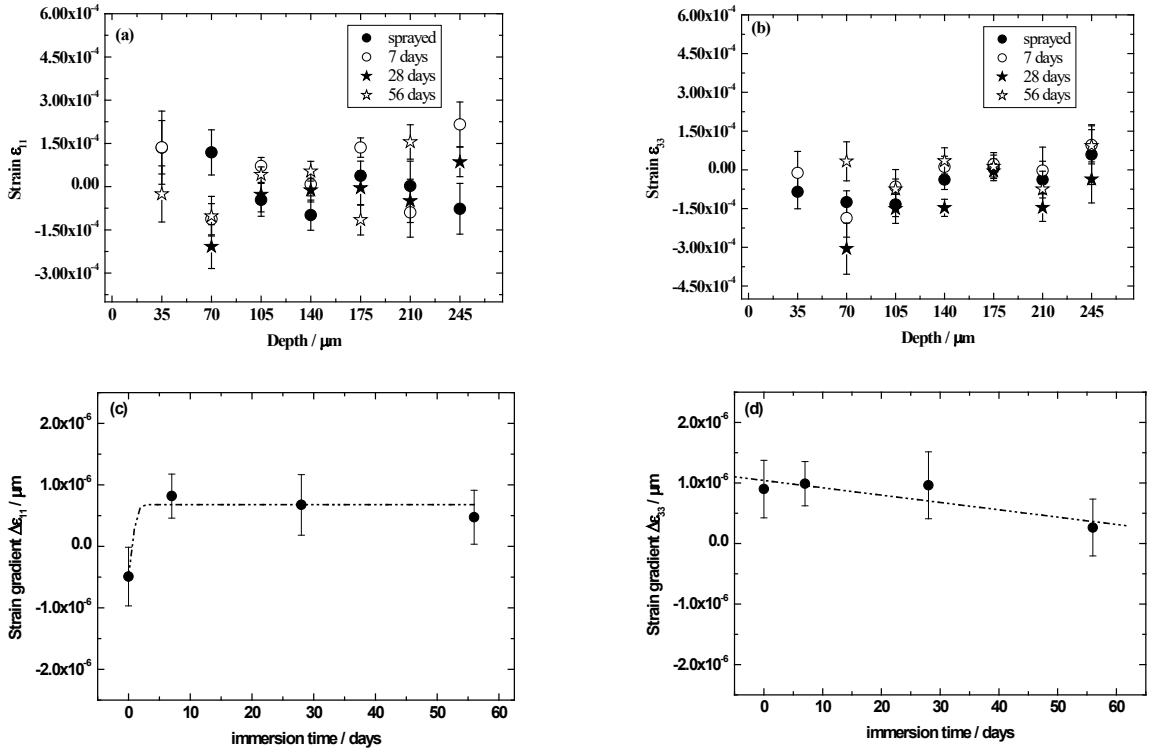

Fig. 3: Variation of strain ε_{ij} and strain gradient $\Delta\varepsilon_{ij}$ with depth and immersion time: a) ε_{11}, b) ε_{33}, c) $\Delta\varepsilon_{11}$, and d) $\Delta\varepsilon_{33}$. (The dotted lines are guides to the eye)

Summary

The effects of simulated body fluids on air-plasma sprayed HAp coatings deposited on flat geometry substrate were investigated employing synchrotron radiation and the following were revealed:

a) Phase identification results showed thermal products to be present throughout the coating of the as-sprayed sample with CaO amongst the first to dissolve upon immersion in SBF. Quantitative analysis showed HAp to be increasing with immersion while TTCP show an oppotite trend.

b) Both the two strain component slopes $\Delta\varepsilon_{11}$ and $\Delta\varepsilon_{33}$ relax upon immersion in SBF with the former showing significant changes within the first 7 days of immersion and stabilising with further immersion time. The latter relaxes linearly with immersion reaching strain free after 56 days.

Acknowledgements

Use of the Advanced Photon Source (APS) at Argonne National Laboratory (ANL) was supported by the U.S. DOE under Contract No. DE-AC02-06CH11357. The authors are indebted to Mrs Margitta Hengst, Department of Mineralogy, Technische Universität Bergakademie Freiberg, Germany for sample preparation, Drs Douglas Robinson and Jonathan Almer, ANL/APS for assisting with the experimental set-up and data acquisition and analysis, respectively as well as Mr. Ryno van der Merwe, for microscopy analysis. The research work was sponsored by the German Federal Ministry of Education and Research (BMBF) and the National Research Foundation of the Republic of South Africa within the research project "Characterisation and determination of residual stress in bioactive coatings and layered structure" (Project code 39.6.G0B.6.A).

References

[1] T. Yamamoto, T. Onga, T. Marui and K. Mizuno, Use of hydroxyapatite to fill cavities after excision of benign bone tumours, J. Bone Joint Surg. (Br.) 82B (2000) 1117.

[2] R.G.T. Geesink, K. de Groot and C.P.A.T. Klein, Chemical implant fixation using hydroxyl-apatite coatings The development of a human total hip prosthesis for chemical fixation to bone using hydroxyl-apatite coatings on titanium substrates, Clin. Orthop. Relat. Res. 225 (1987) 147.

[3] K. de Groot, R. Geesink, C.P.A.T. Klein and P. Serekian, Plasma sprayed coatings of hydroxylapatite, J. Biomed. Mater. Res. 21 (1987) 1375. https://doi.org/10.1002/jbm.820211203

[4] R.B. Heimann and H.D. Lehmann, Bioceramic Coatings for Medical Implants Bioceramic Coatings for Medical Implants. Trends and Techniques. Wiley-VCH, Weinheim, Germany. (2015) 467 pp. 113. https://doi.org/10.1002/9783527682294

[5] R.B. Heimann, Thermal spraying of biomaterials, Surf. Coat. Technol., 201 (2006) 2012. https://doi.org/10.1016/j.surfcoat.2006.04.052

[6] M. Topić, T. Ntsoane, T. Hüttel and R.B. Heimann, Microstructural characterisation and stress determination in as-plasma sprayed and incubated bioconductive hydroxyapatite coatings, Surf. Coat. Technol. 201(6) (2006) 3633. https://doi.org/10.1016/j.surfcoat.2006.08.139

[7] K.A. Gross, C.C. Berndt and H. Herman, Amorphous phase formation in plasma-sprayed hydroxyapatite coatings, J. Biomed. Mater. Res. 39 (1998) 407. https://doi.org/10.1002/(SICI)1097-4636(19980305)39:3%3C407::AID-JBM9%3E3.0.CO;2-N

[8] P. Ducheyne, S. Radin and L. King, The effect of calcium phosphate ceramic composition and structure on in vitro behavior. I. Dissolution, J. Biomed. Mater. Res. 27 (1993) 25. https://doi.org/10.1002/jbm.820270105

[9] TP Ntsoane, M. Topic, M. Härting, R.B. Heimann and C. Theron, Spatial and depth-resolved studies of air plasma-sprayed hydroxyapatite coatings by means of diffraction techniques: Part I, Surf. Coat. Technol. 294 (2016) 153-183. https://doi.org/10.1016/j.surfcoat.2016.03.045

[10] T. Kokubo, H. Kushitani, S. Sakka, T. Kitsugi and T. Yamamuro, Solutions able to reproduce in vivo surface-structure changes in bioactive glass-ceramic A-W, J. Biomed. Mater. Res. 24 (1990) 721-734. https://doi.org/10.1002/jbm.820240607

[11] TOPAS 4.2 2009 Bruker AXS.

[12] J. Almer and U. Lienert, Unpublished document for the Neutron/Synchrotron Summer School, Argonne National Laboratory, 2001.

[13] B. Cofino, P. Fogarassy, P. Millet and A. Lodino, Thermal residual stresses near the interface between plasma-sprayed hydroxyapatite coating and titanium substrate: Finite element analysis and synchrotron radiation measurements, J. Biomed. Mater. Res. (2004) 1-70. https://doi.org/10.1002/jbm.a.30044

[14] A.R. Nimkerdphol, Y. Otsuka and Y. Mutoh, Effect of dissolution/precipitation on the residual stress redistribution of plasma-sprayed hydroxyapatite coating on titanium substrate in simulated body fluid (SBF), J. Mech. Behav. Biomed Mater. 36 (2014) 98-109. https://doi.org/10.1016/j.jmbbm.2014.04.007